available at www.sciencedirect.com

www.elsevier.com/locate/matchar

Dissociation of misfit and threading dislocations in $Ba_{0.75}Sr_{0.25}TiO_3$ epitaxial film

Y.Q. Wang[a,*], *W.S. Liang*[a], *Peter Kr. Petrov*[b], *Neil McN. Alford*[b]

[a]*The Cultivation Base for State Key Laboratory, Qingdao University, No. 308 Ningxia Road, Qingdao, 266071, PR China*
[b]*Department of Materials, Imperial College London, London, SW7 2AZ, United Kingdom*

ARTICLE DATA

Article history:
Received 2 December 2010
Received in revised form
6 January 2011
Accepted 8 January 2011

Keywords:
Epitaxial growth
Microstructure
Electron microscopy
Defects

ABSTRACT

$Ba_{0.75}Sr_{0.25}TiO_3$ film was epitaxially grown on a (001) $LaAlO_3$ substrate using single-target pulsed laser deposition. The dissociation of misfit and threading dislocations in the epitaxial $Ba_{0.75}Sr_{0.25}TiO_3$ film was investigated using high-resolution transmission electron microscopy (HRTEM). For a misfit dislocation with a Burgers vector of [200], it was shown that it could dissociate into four partial dislocations with Burgers vector of type 1/2 <110>. For the threading dislocations, it was found that they usually coexist with stacking faults. The formation mechanism for the dissociated dislocations was discussed. All the dislocations can relieve the local strain in the $Ba_{0.75}Sr_{0.25}TiO_3$ epitaxial film.

1. Introduction

Perovskite barium strontium titanate (Ba, Sr)TiO_3 (BSTO) thin films are a promising candidate for passive microwave components and dynamic random access memory due to their excellent ferroelectric and dielectric properties[1–4]. Extensive research work has indicated that the ferroelectric and dielectric properties of epitaxial BSTO thin film strongly depend on internal stress and defect structure [5–8]. For BSTO thin films grown on a single-crystalline substrate such as $LaAlO_3$ (LAO), there is a lattice mismatch of about 3.8% which could lead to the formation of dislocations, stacking faults (SFs) and antiphase domains in the epitaxial film. These defects could increase the dielectric loss and reduce the tuneability of the film [9]. Thus, it is necessary to carry out a comprehensive investigation of the defect structures, especially the nature of dislocations in epitaxial BSTO films.

In epitaxial perovskite thin films, edge type threading or misfit dislocations with a Burgers vector of **b**=<100> or <110> have been observed in BSTO films grown on $SrTiO_3$ [10–12]. It has been found that the misfit or threading dislocations can dissociate into partial dislocations connected by a strip of stacking faults [12].However, for BSTO/LAO system, few experimental studies are available concerning the mechanism of misfit accommodation and generation of microstructural defects.

In this paper, we report a detailed investigation of the dislocations in the $Ba_{0.75}Sr_{0.25}TiO_3$ film epitaxially grown on a (001) $LaAlO_3$ substrate using high-resolution transmission electron microscopy (TEM). The dissociation and the formation mechanism of misfit and threading dislocations have been studied.

2. Experimental

A 1-μm-thick film of $Ba_{0.75}Sr_{0.25}TiO_3$ was epitaxially grown on a (001) $LaAlO_3$ substrate using a single-target pulsed laser deposition (PLD) technique. Targets for the PLD system were made from ceramic powder prepared using a mixed oxide

---

[*] *Corresponding author*. Tel.: +86 532 83780318.
E-mail address: yqwang@qdu.edu.cn (Y.Q. Wang).

1044-5803/$ – see front matter © 2011 Elsevier Inc. All rights reserved.
doi:10.1016/j.matchar.2011.01.010

route [13]. The epitaxial films were grown on a 5×5 mm^2 $LaAlO_3$ substrate by laser ablation, and the substrate temperature was kept at 650 °C during the deposition. The film thickness was controlled by the number of pulses shot on the targets. Once the ablation was over, the samples were annealed for 1 h in an oxygen rich environment (760 Torr) in order to reduce the oxygen vacancies, and then slowly cooled down to room temperature at a rate of 10 °C/min. The specimens for TEM examination were prepared in a cross-sectional orientation ([010] zone-axis for the $LaAlO_3$ substrate) using conventional techniques of mechanical polishing and ion thinning. The ion milling was performed using a Gatan Model 691 Precision Ion Polishing System (PIPS). The bright-field (BF) imaging, dark-field (DF) imaging, selected-area electron diffraction (SAED) and HRTEM examinations were carried out using a JEOL JEM 2100F transmission electron microscope operating at 200 kV.

3. Results and Discussion

Fig. 1(a) is a typical BF TEM image, while Fig. 1(b) is the corresponding DF TEM image of a cross-sectional $Ba_{0.75}Sr_{0.25}TiO_3$/$LaAlO_3$ sample. These diffraction contrast images were taken under a two-beam condition with g = 002. It can be seen from Fig. 1(a) and (b) that the density of dislocations is higher in the region near the $Ba_{0.75}Sr_{0.25}TiO_3$/$LaAlO_3$ interface while a remarkable reduction of the dislocation density takes place in the top layer. Fig. 1(c) is a typical SAED pattern taken from the epitaxial film region, which corresponds to a [010] zone-axis diffraction pattern of $Ba_{0.75}Sr_{0.25}TiO_3$ film, suggesting that the epitaxial $Ba_{0.75}Sr_{0.25}TiO_3$ films are good single crystals. Fig. 1(d) is a typical SAED pattern taken from the interface region between $Ba_{0.75}Sr_{0.25}TiO_3$ film and $LaAlO_3$ substrate. It showed a superposition of $Ba_{0.75}Sr_{0.25}TiO_3$ [010] and $LaAlO_3$ [010] zone-axis electron diffraction patterns. The epitaxial $Ba_{0.75}Sr_{0.25}TiO_3$ film has an interface relationship of $(001)_{BSTO}$//$(001)_{LAO}$ and $[010]_{BSTO}$//$[010]_{LAO}$ with respect to the substrate.

Extensive TEM examinations of the specimen indicated that most of the misfit or threading dislocations are pure-edge types with Burgers vectors of <100> or <101>, and they tend to dissociate into partials with Burgers vectors of type $\frac{1}{2}$ <101>, bound by a strip of SFs.

For the misfit dislocations, they are not exactly located at the $Ba_{0.75}Sr_{0.25}TiO_3$/$LaAlO_3$ interface, but inside the $Ba_{0.75}Sr_{0.25}TiO_3$ film a few monolayers away from the interface. The dissociation of the misfit dislocations happens near the interface between $Ba_{0.75}Sr_{0.25}TiO_3$ and $LaAlO_3$. One example is shown in Fig. 2(a). Careful examination of Fig. 2(a) demonstrates that there are two extra half planes along the $[10\bar{1}]$ direction, and another two extra half planes along the [101] direction, indicating that they belong to pure-edge type dislocation. The extra half planes are indicated by dashed lines for D1, D2, D3 and D4 in Fig. 2(a). The dislocations line direction for D1, D2, D3, D4 is along [010]. To determine the Burgers vectors for the dislocations, Burgers circuits are drawn to enclose the dislocations in the enlarged HRTEM images of rectangle regions in Fig. 2(a). The Burgers vectors for D1 and D2 are the same, so only one Burgers circuit is drawn in Fig. 2(b). It can be clearly seen from Fig. 2(b) that there is a gap between the starting and ending point in each Burgers circuit, which is indicated by an arrow. The Burgers vectors for dislocations D1 and D2 are both determined to be $\frac{1}{2}$ $[10\bar{1}]$. For the D3 and D4, because the Burgers vectors are the same, one Burgers circuit is drawn in Fig. 2(c). The Burgers vectors for dislocations D3 and D4 are both determined to be $\frac{1}{2}$[101]. The four partials in Fig. 2(a) belong to a dissociated edge misfit dislocation according to the reaction as follows

$$[200] \rightarrow \frac{1}{2}[10\bar{1}] + \frac{1}{2}[10\bar{1}] + \frac{1}{2}[101] + \frac{1}{2}[101]. \qquad (1)$$

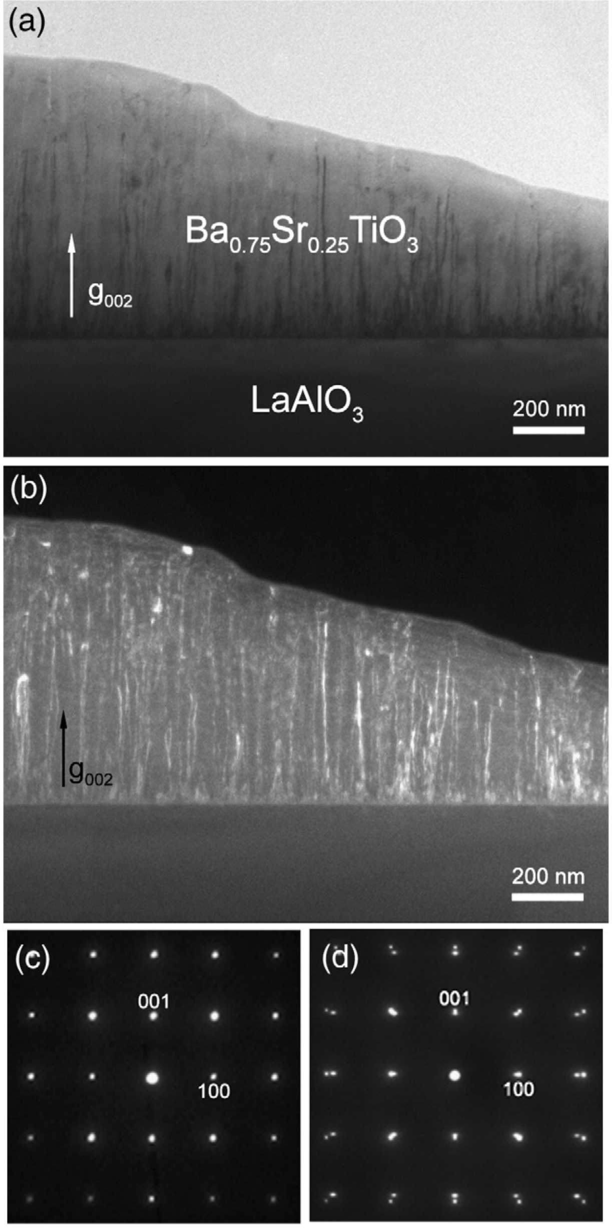

Fig. 1 – Cross-sectional BF (a) and DF (b) TEM image of $Ba_{0.75}Sr_{0.25}TiO_3$/$LaAlO_3$ taken near the [010] zone axis with a diffraction vector of g = 002; (c) typical [010] zone-axis SAED pattern taken from the epitaxial film; (d) typical [010] zone-axis SAED pattern from the interface region.

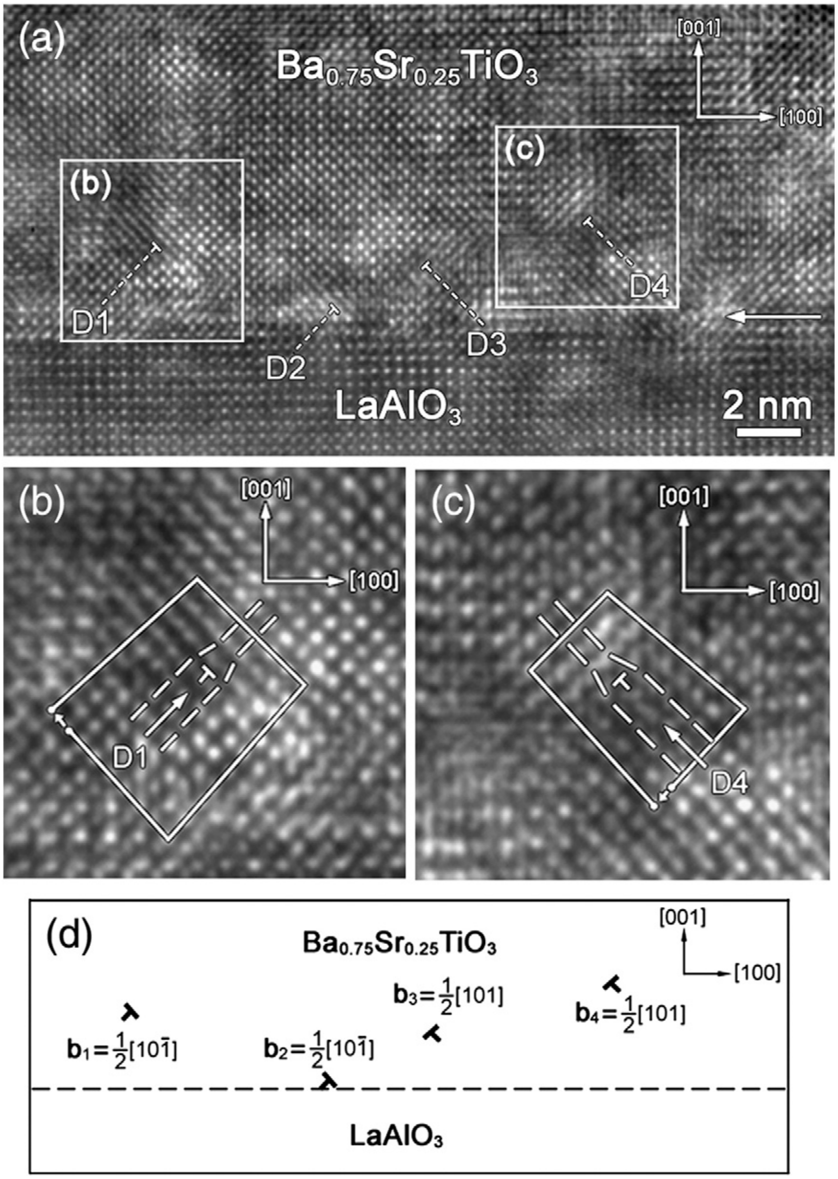

Fig. 2 – (a) An example of misfit dislocation dissociated into four partials; Burgers circuit for partials D1 and D2 (b); D3 and D4 (c); (d) schematic diagram for the dissociation of misfit dislocation.

In reaction (1), there is no change in dislocation energy from left to right. However, three stacking faults are unavoidably generated between the partial dislocations, increasing the energy of the configuration. Despite of the unfavourable energy balance, this dissociation may occur under special conditions where large strains exist in the interfacial region of the films or nonstoichiometry needs to be accommodated (effectively a negative energy stacking fault). Fig. 2(d) is a schematic diagram of the four partials. All the partials can contribute to the misfit relaxation because they have edge components parallel to the interface plane. During the PLD process, island growth dominates due to large lattice mismatch between $LaAlO_3$ and $Ba_{0.75}Sr_{0.25}TiO_3$. With further growth of the strained $Ba_{0.75}Sr_{0.25}TiO_3$ islands, dislocations were generated near the edges of the islands. Some dislocations were formed as perfect dislocations and the others as partials bound by stacking faults.

For the threading dislocations, it has been found that they tend to dissociate into partials bound by stacking faults. Fig. 3(a) shows an example of a partial bound by a strip of stacking faults. Usually a threading dislocation is dissociated into two partials bound by stacking faults. Here only one partial is observed to connect with stacking faults. The possible reason is that the other one near the free surface of the sample disappeared during the ion milling process. In order to determine the Burgers vector, the Burgers circuit is drawn in the enlarged HRTEM image shown in Fig. 3(b). The enlarged HRTEM image of the stacking faults is shown in Fig. 3(c). It can be seen that there is a gap between the starting and ending point, which is indicated by an arrow. The Burgers vector for this partial dislocation is

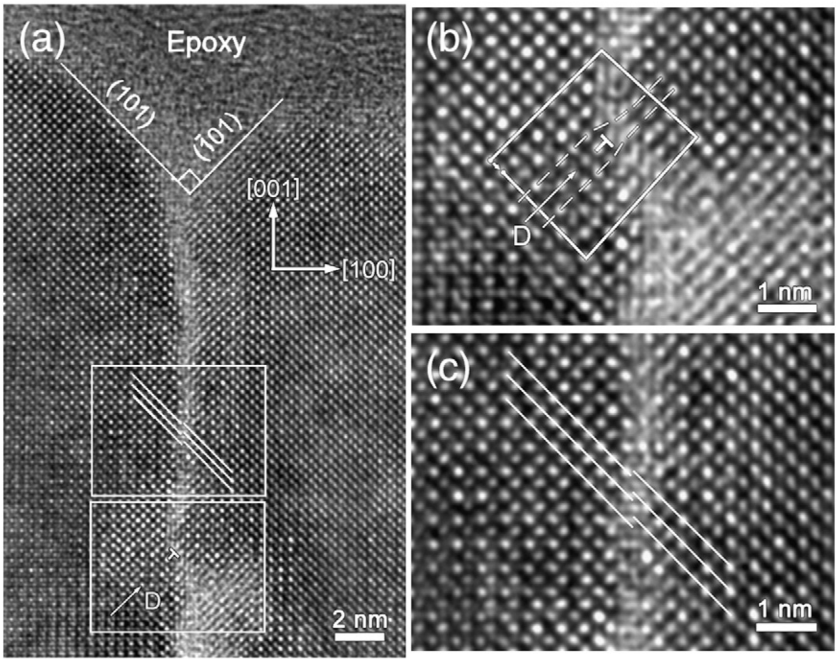

Fig. 3 – (a) An example of dissociation of a threading dislocation; (b) Burgers circuit for the partial dislocation; (c) enlarged HRTEM image showing the lattice displacement.

determined to be $\frac{1}{2}$ [101]. The threading dislocation is formed during the coalescence of the neighbouring islands in order to relieve the local strain.

4. Conclusions

In conclusion, the misfit and threading dislocations were investigated using HRTEM technique. A misfit dislocation with a Burgers vector of [200] is observed to dissociate into four partials with Burgers vector of type 1/2 <110>. A threading dislocation is observed to dissociate into two partials bound by a strip of stacking faults, while only one partial is observed. All the dislocations can relieve the local strain in the $Ba_{0.75}Sr_{0.25}TiO_3$ epitaxial film.

Acknowledgements

The authors would like to thank the financial support from the National Natural Science Foundation of China (Grant no.10974105), the Scientific Research Starting Foundation for the Introduced Talents at Qingdao University (Grant No. 06300701) and Taishan Outstanding Overseas Scholar Program of Shandong Province. The authors are grateful to Prof. Xiaofeng Duan at Institute of Physics, Chinese Academy of Sciences for his helpful discussion.

REFERENCES

[1] Zafar S, Jones RE, Jiang B, White B, Chu P, Taylor D, et al. The electronic conduction mechanism in barium strontium titanate thin films. Appl Phys Lett 1998;73:175–7.

[2] Cho HJ, Oh SJ, Kang CS, Hwang CS, Lee BT, Lee KH, et al. Improvement of leakage current characteristics of $Ba_{0.5}Sr_{0.5}TiO_3$ films by N_2O plasma surface treatment. Appl Phys Lett 1997;71:3221–3.

[3] Dietz GW, Schumacher M, Waser R, Streiffer SK, Basceri C, Kingon AI. Leakage currents in $Ba_{0.7}Sr_{0.3}TiO_3$ thin films for ultrahigh-density dynamic random access memories. J Appl Phys 1997;82:2359–64.

[4] Hwang CS, Joo SH. Variations of the leakage current leakage density and the dielectric constant of Pt/(Ba, Sr)TiO3/Pt capacitors by annealing under a N2 atmosphere. J Appl Phys 1999;85:2431–6.

[5] Hyun S, Lee JH, Kim SS, Char K, Park SJ, Sok J, et al. Anisotropic tuning behaviour in epitaxial $Ba_{0.5}Sr_{0.5}TiO_3$ thin films. Appl Phys Lett 2000;77:3084–6.

[6] Taylor TR, Hansen PJ, Acikel B, Pervez N, York RA, Streiffer SK, et al. Impact of thermal strain on the dielectric constant of sputtered barium strontium titanate thin films. Appl Phys Lett 2002;80:1978–80.

[7] Ban ZG, Alpay SP. Optimization of the tunability of barium strontium titanate films via epitaxial stresses. J Appl Phys 2003;93:504–11.

[8] Pertsev NA, Zembilgotov AG, Tagantsev AK. Effect of mechanical boundary conditions on phase diagrams of epitaxial ferroelectric thin films. Phys Rev Lett 1998;80:1988–91.

[9] Lu CJ, Bendersky LA, Chang K, Takeuchi I. High-resolution identification of 1/2 <110> stacking faults in epitaxial $Ba_{0.3}Sr_{0.7}TiO_3$ thin films. Phil Mag 2003;83(13):1565–86.

[10] Qi XY, Miao J, Duan XF, Zhao BR. Threading dislocations in $Ba_{0.7}Sr_{0.3}TiO_3/La_{0.7}Sr_{0.3}TiO_3$ epitaxial films grown on (001) $LaAlO_3$ substrate. Mater Lett 2006;60:2009–12.

[11] Qi XY, Miao J, Duan XF, Zhao BR. Microstructure of $La_{0.7}Sr_{0.3}TiO_3/Ba_{0.7}Sr_{0.3}TiO_3/La_{0.7}Sr_{0.3}MnO_3$ epitaxial films grown on (001) $SrTiO_3$ substrate. J Cryst Growth 2005;277:218–22.

[12] Suzuki T, Nishi Y, Fujimoto M. Analysis of misfit relaxation in heteroepitaxial $BaTiO_3$ thin films. Philos Mag A 1999;79:2461–83.

[13] Sarma K, Farooq R, Jarman K, Pullar R, Petrov PK, Alford NM. Sintering behaviour of $Ba_xSr_{1-x}TiO_3$. Integr Ferroelectr 2004;62:249.